Full length article

Insight into the uptake and metabolism of a new insecticide cyetpyrafen in plants

Runan Li [a], Sijia Wang [a], Jinhe Chang [a], Xinglu Pan [a], Fengshou Dong [a], Zhiyuan Li [b], Yongquan Zheng [a], Yuanbo Li [a,*]

[a] State Key Laboratory for Biology of Plant Diseases and Insect Pests, Institute of Plant Protection, Chinese Academy of Agricultural Sciences, Beijing 100193, PR China
[b] Shanghai AB Sciex Analytical Instrument Trading Co, Ltd, Beijing 100015, PR China

ARTICLE INFO

ABSTRACT

As new agrochemicals are continuously introduced into agricultural systems, it is essential to investigate their uptake and metabolism by plants to better evaluate their fate and accumulation in crops and the subsequent risks to human exposure. In this study, the uptake and elimination kinetics and transformation of a novel insecticide, cyetpyrafen, in two model crops (lettuce and rice) were first evaluated by hydroponic experiments. Cyetpyrafen was rapidly taken up by plant roots and reached a steady state within 24 h, and it was preferentially accumulated in root parts with root concentration factors up to 2670 mL/g. An uptake mechanism study suggested that root uptake of cyetpyrafen was likely to be dominated by passive diffusion and was difficult to transport via xylem and phloem. Ten phase I and three phase II metabolites of cyetpyrafen were tentatively identified in the hydroponic-plant system through a nontarget screening strategy. The structures of two main metabolites (M-309 and M-391) were confirmed by synthesized standards. The metabolic pathways were proposed including hydroxylation, hydrolysis, dehydrogenation, dehydration and conjugation, which were assumed to be regulated by cytochrome P450, carboxylesterase, glycosyltransferase, glutathione S-transferases and peroxidase. Cyetpyrafen and its main metabolites (M-409, M-309 and M-391) were estimated to be harmful/toxic toward nontarget organisms by theoretical calculation. The high bioaccumulation and extensive transformation of cyetpyrafen highlighted the necessity for systematically assessing the crop uptake and metabolism of new agrochemicals.

1. Introduction

The development and application of new pesticides not only provide more options for plant disease/insect control but could also mitigate pesticide resistance development in agricultural practices. However, after release into the environment, the potential risks of these new chemicals to human health and ecosystems are rising great public concerns (Naidu et al., 2021). For instance, Shao et al. (2022) recently reported that the novel vanillin-derived pesticide vanisulfane could cause hepatic steatosis in both sexes of rats and mild gonadal effects in males. The novel neonicotinoid cycloxaprid was found to be extensively transformed in crops and the environment (Cheng et al., 2022; Shen et al., 2021), where its main metabolite 2-chloro-5-[(2-(nitromethylene)-1-imidazolidinyl)methyl]pyridine possessed higher toxicity toward honeybees and mice than its parent form (Shao et al., 2013). Cyetpyrafen (Fig. S1) is a novel pyrazole insecticide with a broad spectrum of insecticidal/acaricidal activity that can effectively control

pests such as *Thrips hawaiiensis, Tetranychus cinnabarinus* and *Tetranychus urticae* in horticultural and agricultural crops (Li et al., 2020a; Lin et al., 2021; Ouyang et al., 2018). Similar to the pyrazole insecticide cyenopyrafen, cyetpyrafen inhibits complex II of the mitochondrial electron transport chain after hydrolysis of its ester bond to the bioactive product in pests (Khalighi et al., 2014). As a new pesticide, the existing research on cyetpyrafen mainly focused on its bioactivity (Yu et al., 2016), toxicity to natural predators (Feng et al., 2021), resistance to spider mites (Chen et al., 2019) and exposure risk assessment for occupational handlers (Wang et al., 2020). The effective and safe application of a new pesticide demands thorough knowledge of its fate and metabolism in plants, as these are essential information in evaluating food safety and potential human exposure via dietary intake. However, to date, there are no data available concerning the uptake and metabolism of cyetpyrafen in plants.

A large proportion of pesticides (e.g., > 80 %) enter the soil and water after application (Aktar et al., 2009). Understanding plants take

up and transport a new pesticide from soil (or water) is important in assessing its potential accumulation and in-plant distribution (Ju et al., 2020). Pesticides in soils move into plants primarily through root uptake and are subsequently transported to other parts through xylem and phloem (Miller et al., 2016; Sicbaldi et al., 1997). Root uptake of pesticides is mainly recognized as a passive diffusion process (Malchi et al., 2021). However, some studies also found that active uptake (e.g., protein-mediated energy-dependent uptake) might also be involved in the root uptake of pesticides and might coexist with the passive uptake process. For example, Fu et al. (2016) demonstrated that a transporter-mediated active uptake process was involved in the uptake of roxarsone by wheat seedlings. Nevertheless, few studies have tried to elucidate the uptake pathways of new pesticides by plant roots. In addition, phloem transport is an important pathway in distributing pesticides throughout plant tissues from leaves to roots, fruits and buds (Chen et al., 2021; Liu et al., 2019). For example, glyphosate was found to be effectively transported in the phloem of castor bean plants (Bromilow et al., 1993). The phloem mobility of pesticides in crops affects their efficacy and the potential edible part accumulation (e.g., fruits). However, the role of phloem in the translocation of pesticides has also not been well explored. Therefore, a mechanistic understanding of the uptake and transport of a new pesticide (e.g., cyetpyrafen) is needed to predict plant accumulation.

After being taken up, pesticides can be transformed by plant metabolic processes and exist in the form of metabolites. Metabolic transformation of pesticides by plants usually reduces their toxicity (Van Eerd et al., 2003). However, in some cases, plant transformation may yield metabolites that are even more toxic than parent pesticides (Miller et al., 2016; Shen et al., 2021; WildemanNazar, 1982). For instance, prothioconazole-desthio is a main metabolite of prothioconazole in plants, which is 3.5 times more toxic than prothioconazole to zebrafish and exhibits higher reproductive toxicity to mammals (Xie et al., 2019; Zhang et al., 2020). In general, the metabolism of pesticides in plants consists of three phases: reactions of phase I metabolism include oxidation, hydrolysis and reduction, which usually generate more water-soluble and reactive products; conjugation reactions with endogenous components in plants (e.g., glutathione, sugar, and amino acids) occur in phase II metabolism; phase III metabolism leads to further compartmentalization of conjugates into the vacuole and apoplast (Coleman et al., 1997; Riemenschneider et al., 2017; Van Eerd et al., 2003). Many plant enzymes participate in catalyzing pesticide metabolism, including cytochrome P450 (CYP450), peroxidase (POD), carboxylesterase (CarE), glycosyltransferase (GT) and glutathione *S*-transferases (GST). (Van Eerd et al., 2003). As a result, plant transformation of pesticides may impact their efficacy, extent of plant uptake, and potential human exposure. However, the metabolic pathways of many novel pesticides in plants are still largely unknown and poorly predicted (Hurtado et al., 2016). Therefore, elucidating the main metabolites and understanding the mechanism of metabolism of pesticides in plants is essential for accurate risk assessment, registration and risk control of a new pesticide such as cyetpyrafen.

Due to the lack of understanding of the fate of the new pesticide cyetpyrafen in crop systems, it is difficult to predict effective plant accumulation and overall toxicity which are important in assessing its potential environmental and health risks. To fill the information gap, the uptake, bioaccumulation and transformation of cyetpyrafen in two model crops (lettuce and rice) as well as the relevant mechanism were investigated. The plant uptake and translocation mechanisms were explored by adding different inhibitors and performing a split-root test. A total of 13 new metabolites were first identified in the hydroponic-plant system through a nontarget screening strategy by using liquid chromatography (LC) with high-resolution mass spectrometry (HRMS), and the metabolic pathways and plant enzymes involved in the processes were further explored. Moreover, the nontarget toxicities of cyetpyrafen as well as the identified metabolites were assessed by a computerized predictive system. The results from this study could contribute mechanistic insight into the uptake and metabolism of novel pesticides in plants, which provide basic information for safety assessment and further registration of these chemicals, such as cyetpyrafen.

2. Materials and methods

2.1. Chemicals and reagents

Cyetpyrafen (purity: 98.4 %) was supplied by Shenyang Sinochem Agrochemicals R&D Co., Ltd. (Shenyang, China). Authentic standards of metabolites, including M-391 (purity: 99.5 %) and M-309 (purity: 99.5 %), were synthesized by our lab. Plant CYP450 enzyme-linked immunosorbent assay (ELISA) kit, plant POD ELISA kits, plant CarE ELISA kits, plant GT ELISA kits and plant GST ELISA kits were purchased from Shanghai Enzyme-linked Biotechnology Co., Ltd. (Shanghai, China). Other details of the chemicals and reagents are shown in S1 in the Supplementary material.

2.2. Plant uptake and depuration experiments

Rice (*Oryza sativa Japonia cv. Nipponbare*) and lettuce seeds (*Lactuca sativa*) were sterilized in 2–3 % sodium hypochlorite solution for 10 min. Afterward, the seeds were washed with deionized water three times. Seed germination was performed in seeding plates at 23–25 °C. Then, uniform-size seedlings were transferred into 1 L glass containers (each container had 24 rice seedlings or 2 lettuce seedlings) with Yamazaki's nutrient solution (pH = 5.8). The glass containers were all wrapped with foil paper to avoid potential photolysis. The relative humidity was maintained at 60–70 % with a light:dark cycle of 14:10 h. After 30 days of growth, the plants were transferred to 1 L glass containers containing 1 L of nutrient solution. The nutrient solution was fortified with cyetpyrafen at 1 mg/L (actual measured concentration was 1.12 mg/L) for the exposure experiment. Two controls were included: a plant-free control (solution with cyetpyrafen only) to monitor the loss of cyetpyrafen and a pesticide-free control (plant only). All exposure and control experiments were performed in triplicate. During the exposure experiment, 40–90 mL fresh nutrient solution (without cyetpyrafen) was added to each container daily to compensate for the plant transpiration loss (Fig. S2).

To assess the plant accumulation kinetics, plant (24 rice seedlings or 2 lettuce seedlings were collected as one sample) and nutrient solution samples were collected at 1, 3, 6, 10, 24, 48, 72 and 96 h. At the end of the exposure, all the remaining plants were removed from the containers, and the roots were thoroughly washed with deionized water. Then, the plants were transferred into new glass containers containing 1 L of nutrient solution without pesticide. During the depuration stage, plant and nutrient solution samples were collected at 3, 6, 10, 24 and 72 h after transplanting. The plant samples were rinsed with deionized water, wiped with filter paper, weighed, and separated into shoots and roots. The potential hydrolysis of cyetpyrafen was evaluated by sampling the nutrient solution samples from plant-free containers across the uptake and depuration stages at time intervals of 0, 3, 6, 10, 24, 48, 72, 96, 120 and 168 h. All collected samples were stored at −20 °C prior to analysis.

To assess the plant enzyme response in the plant metabolic process, extra plant samples were collected from the exposure experiment at 24, 48 and 96 h during the plant uptake stage and 72 h the during depuration stage to measure the enzyme activity. Plant samples were stored at −80 °C after quick freezing with liquid nitrogen. Briefly, 1 g of root samples (fresh weight) was homogenized on ice with 9 mL phosphate buffered saline (PBS) solution (0.01 mol/L, pH = 7.2–7.4). The homogenate was centrifuged at 4000 rpm for 15 min (4 °C), and the supernatant was collected for analyzing enzyme activities by plant enzyme ELISA kits. CYP450, CarE, GT, GST and POD enzyme activities were measured using a spectrophotometer (RT-6100 Microplate Reader, Rayto) at a wavelength of 450 nm. The enzyme activities were denoted

as U/g protein. Details of the enzyme assays are shown in S2.

2.3. Effect of inhibitors on plant uptake

To clarify the uptake mechanisms, the influences of metabolic, aquaporin, and anion-channel inhibitors on root uptake of cyetpyrafen were evaluated. Six groups of tests were performed, which were similar to the plant uptake experiment. Each group contained three replicates, and the exposure concentration of cyetpyrafen was set at 1 mg/kg. A group without inhibitors was used as a control. Briefly, 0.5 mmol/L of sodium vanadate (NaV_3O_4) was applied as a metabolic inhibitor (Li et al., 2017), 1 mmol/L of glycerol and 1 μmol/L of $AgNO_3$ were selected as aquaporin inhibitors, and 10 μmol/L of anthracene-9-carboxylic acid (9-AC) and 5 μmol/L of 4, 4′-diisothiocyano-2,2′-stilbenedisulfonate (DIDS) were used as anion channel inhibitors (Gong et al., 2020). After 6 h of exposure, all plant roots were rinsed with deionized water, wiped with filter paper, collected and stored at −20 °C.

2.4. Split-root exposure test

To test whether phloem transport plays a role in the long-range translocation of cyetpyrafen in plants, a split-root test was performed for rice seedlings, as they have fibrous roots compared with lettuce. The split-root exposure test was performed in two PTFE tubes marked as tube A and tube B. Tube A contained 50 mL of nutrient solution with spiked cyetpyrafen at 5 mg/L, and tube B contained the same amount of fresh nutrient solution without cyetpyrafen. The rice seedling roots were separated into two parts, which were linked to the same shoots. The two parts of the roots were put into tube A and tube B separately. Rice seedlings were sampled at 3, 6, 10, 24, 48, 72 and 96 h. Concentrations of cyetpyrafen in the roots and nutrient solutions from both tubes A and B as well as in the shoots were measured. The blank control group was set, and all treatments were conducted in triplicate. The collected samples were stored at −20 °C prior to analysis.

2.5. Sample analysis

The plant samples were freeze-dried at −40 °C for 2 days and homogenized. Initially, 0.2 g of shoots (0.1 g for roots, dry weight) or 1 mL of solution samples were weighed into 10 mL polytetrafluoroethylene (PTFE) centrifuge tubes. Then, 2 mL of ACN was added and vortexed for 10 min with an oscillation frequency of 2500 min^{-1}. Afterward, 0.5 g of NaCl was added to the tubes and vortexed for another 5 min. Subsequently, the tubes were centrifuged at 4000 rpm for 5 min. For nutrient solutions, the upper layer was directly transferred into an autosampler vial by passing through a 0.22-μm PTFE membrane filter. For shoot and root samples, 1.2 mL of the upper layer was transferred into a 2 mL centrifuge tube containing 150 mg anhydrous $MgSO_4$ and sorbents (50 mg PSA + 10 mg GCB for shoots and 50 mg PSA for roots). The tubes were then vortexed for 1 min and centrifuged at 5000 rpm for 5 min. The upper layer was also filtered through a 0.22-μm PTFE membrane filter. The samples were stored at −20 °C before analysis.

2.6. Quantitative analysis and metabolites screening

The cyetpyrafen concentration was quantified using UHPLC-MS/MS; more details are described in S3 and Table S1. Quality control was performed by regular analyses of procedural blanks, and solvent blanks were injected after each batch of 20 samples to monitor the background and instrumental contamination. The matrix-matched calibration standard curves were applied for quantification to minimize the matrix effects (−12.5–12.5 % for all matrices, Table S2). The matrix-matched solutions were prepared at 1, 5, 10, 50, 100, 500 and 1000 μg/L by adding stock solution to blank matrix extractions. The linearity of the calibration curves in the matrix and solvent ranged from 1 μg/L to 1000 μg/L, with correlation coefficients (R^2) ≥ 0.995 (Table S2). The

recoveries and relative standard deviations (RSDs) of the tests were 80.4–108 % and 0.74–15.5 % for all matrices, respectively (Table S3). The method detection limit (MDL) represents the concentration with a signal-to-noise ratio (S/N) equal to 3. The method limit of quantification (LOQ) was determined at the lowest spiked level of the validation meeting the method performance acceptability criteria according to the European Union SANTE/11312/2021 regulatory guidelines. As shown in Table S2, the MDLs and LOQs of cyetpyrafen in all matrices were 0.00526–0.0142 and 1–10 μg/kg (or μg/L), respectively. Other details of the quality assurance and quality control are shown in S4.

To identify possible metabolites, plant and nutrient solution extracts were analyzed on an ExionLC™ AD System coupled with a TripleTOF® 5600$^+$ System (AB SCIEX, United States). The system was equipped with an electrospray ionization (ESI) source which was operated in positive ion mode. Chromatographic separation was accomplished on an ACQUITY UPLC HSS T3 column (2.1 mm × 100 mm, 1.8 μm) with a gradient elution program using Milli-Q water (containing 0.1 % of formic acid) and acetonitrile as the mobile phase. The main TOF-MS parameters are provided in S5. The acquired data, including mass spectra (MS) and MS/MS information, were analyzed by MetabolitePilot™ 2.0 software (AB SCIEX, United States). A binary comparison strategy was adopted to screen the potential metabolites, and chromatograms of cyetpyrafen and metabolite candidates were identified in cyetpyrafen-treated samples by comparison with controls in terms of sample/control ratios higher than 3. The minimum peak intensities of TOF MS and TOF MS/MS were set as 5000 and 1000 counts per second (cps), respectively. The MS m/z tolerance was set lower than 5 parts per million (ppm). The MS library of cyetpyrafen was established containing the structure and its characteristic fragments. Phase I and phase II metabolic pathways, such as oxidation, hydrolysis and conjugation reactions, were added to the software. Then, the structures of potential transformation products were deduced based on the individual accurate mass (m/z), fragment ions, fragmentation patterns and biotransformation knowledge of xenobiotics.

2.7. Ecotoxicity evaluation

The chronic and acute ecotoxicity of cyetpyrafen and its metabolites were evaluated by ECOSAR (Ecological Structure Activity Relationships) (Version 1.11). The program was developed by the United States Environmental Protection Agency (EPA) and Syracuse Research Corporation (SRC). The acute toxicity of cyetpyrafen and its metabolites to fish was represented as the median lethal concentration (LC_{50}), and toxicity to daphnid and green algae was expressed as the median effective concentration (EC_{50}). The classification of ecotoxicity is described in S6.

2.8. Data analysis

The dissipation dynamics of cyetpyrafen in nutrient solution were estimated by the first-order kinetic equation (Ju et al., 2020):

$$C_t = C_0 \times e^{-k1t} \tag{1}$$

where C_0 and C_t are the concentrations (μg/L) of cyetpyrafen in the nutrient solution at time 0 h and t, respectively, and k_1 is the dissipation rate constant (per hour).

The accumulation kinetics of cyetpyrafen by plants in 96 h plant uptake experiments were fitted according to the first-order one-compartment model with the following equations (Liu et al., 2019):

$$C_t = C_{eq}(1 - e^{-k2t}) \tag{2}$$

where C_{eq} and C_t are the concentration (μg/kg, dw) of cyetpyrafen in plant tissues at uptake equilibrium and time t, respectively, and k_2 represents the uptake rate constant (per hour).

The elimination kinetics of cyetpyrafen by plants in 72 h depuration experiments were measured by the pseudo-first-order decay model (Liu

et al., 2019):

$$C_t = (C_0 - Y)e^{-k_3t} + Y \tag{3}$$

where C_0 and C_t are the concentrations (μg/kg, dw) of cyetpyrafen in plant tissues at time 0 h and time t during the depuration stage, respectively; k_3 represents the elimination rate constant (per hour); and Y is the plateau concentration (μg/kg, dw).

The dissipation half-life ($T_{1/2}$) of cyetpyrafen in nutrient solution (k_1) during 96 h plant uptake experiments and elimination half-lives of cyetpyrafen in roots/shoots (k_3) during 72 h depuration experiments were calculated as follows (Liu et al., 2019):

$$T_{1/2} = ln2/k \tag{4}$$

The root concentration factor (RCF) and translocation factor (TF) were calculated by the following equations:

$$RCF = C_{root}/C_{solution} \tag{5}$$

$$TF = C_{shoot}/C_{root} \tag{6}$$

where C_{root}, C_{shoot} and $C_{solution}$ represent the concentrations of cyetpyrafen in root (μg/kg, dw), shoot (μg/kg, dw) and nutrient solution (μg/L), respectively. Statistical analysis was performed by SPSS Statistics (version 17.0, IBM Corp., Armonk, NY). One-way analysis of variance (ANOVA) followed by Duncan's test was used to analyze the significant difference between the data of two groups at three significance levels (*$P < 0.05$, **$P < 0.01$, ***$P < 0.001$).

3. Results and discussion

3.1. Accumulation and elimination kinetics of cyetpyrafen in rice and lettuce

As shown in Fig. 1A, the accumulation kinetics of cyetpyrafen by both plant roots were well fitted to a first-order kinetic model ($R^2 \geq 0.716$, Table S4). The kinetic rate constants originated from both the uptake and transformation processes of cyetpyrafen. The uptake process could be separated into two phases, that is, a fast process reaching steady state within 24 h followed by a lag phase (24–96 h) (Fig. 1A). Cyetpyrafen exhibited a faster uptake rate in lettuce roots ($k_{2, roots}$, 0.301 h^{-1}) than in rice roots ($k_{2, roots}$, 0.218 h^{-1}), and its concentration in lettuce roots was greater than that in rice roots at each sampling point during 96 h of exposure (Fig. 1A). In addition, the results indicated that cyetpyrafen was highly accumulated in plant roots with average RCFs of 1290 mL/g and 1730 mL/g in rice and lettuce, respectively (Table S5,

Fig. S3A), during the uptake equilibrium stage (24–96 h). Again, the bioaccumulation potential of cyetpyrafen in lettuce roots was greater than that in rice roots, suggesting plant species-dependent uptake and bioaccumulation. In contrast, the cyetpyrafen concentrations in both plant shoots followed a very different trend from those in roots, increasing over the 96 h of exposure and not reaching steady state as roots did (Fig. 1B). In addition, cyetpyrafen exhibited much less accumulation in shoots than in roots, as evidenced by the extremely low TFs (e.g., TF $\leq 5.37 \times 10^{-4}$ for rice and $\leq 4.29 \times 10^{-5}$ for lettuce), indicating its poor translocation ability and preferential accumulation in roots (Table S5, Fig. S3B). Cyetpyrafen is a highly lipophilic pesticide (log $K_{ow} = 6.1$, estimated by ECOSAR Version 1.11), which is expected to cross the plasma membrane and sorb to the roots easily, while its translocation to the upper part is difficult (Romeh and Hendawi, 2013; Trapp, 2000). Additionally, the relatively large-sized molecule (molecular weight of cyetpyrafen: 393.5218 g/mol) may also limit its transport from roots to aboveground tissues via the xylem system (Chen et al., 2020; Chuang et al., 2019). Thus, it might take a longer time for cyetpyrafen to reach accumulation equilibrium in shoots.

During the 72 h of depuration period, the quick elimination of cyetpyrafen from roots followed a pseudo-first-order decay model, and the elimination rate in lettuce roots ($T_{1/2}$, 13.5 h) was approximately 4.40 times slower than that in rice roots ($T_{1/2}$, 3.07 h, Fig. 1A). The faster uptake and slower elimination rate may account for the greater accumulation of cyetpyrafen in lettuce than that in rice. Two main pathways could be relevant for root elimination: transformation and mass transfer from roots to aboveground parts or growth media (Qiu et al., 2016). Since the translocation of cyetpyrafen to shoots was extremely limited, its rapid elimination in plant roots was mainly a result of biotransformation and/or release to the surrounding solution. The elimination of cyetpyrafen in both plant shoots exhibited a faster rate ($T_{1/2}$, 0.812–1.00 h) than that in roots (Fig. 1B), suggesting its rapid biotransformation in shoots.

3.2. Uptake mechanism

3.2.1. Effects of inhibitors on root uptake of cyetpyrafen

The uptake mechanism of cyetpyrafen was explored by adding metabolic (NaV_3O_4), aquaporin (glycerol and $AgNO_3$) and anion channel inhibitors (9-AC and DIDS) into the hydroponic system (a detailed discussion is presented in S7). Compared to the control group (without inhibitor), the concentrations of cyetpyrafen in treatment plants by adding the five inhibitors were not significantly reduced (Fig. S4). The results indicated that the root uptake of cyetpyrafen was possibly through a passive diffusion process, in which aquaporin and anion
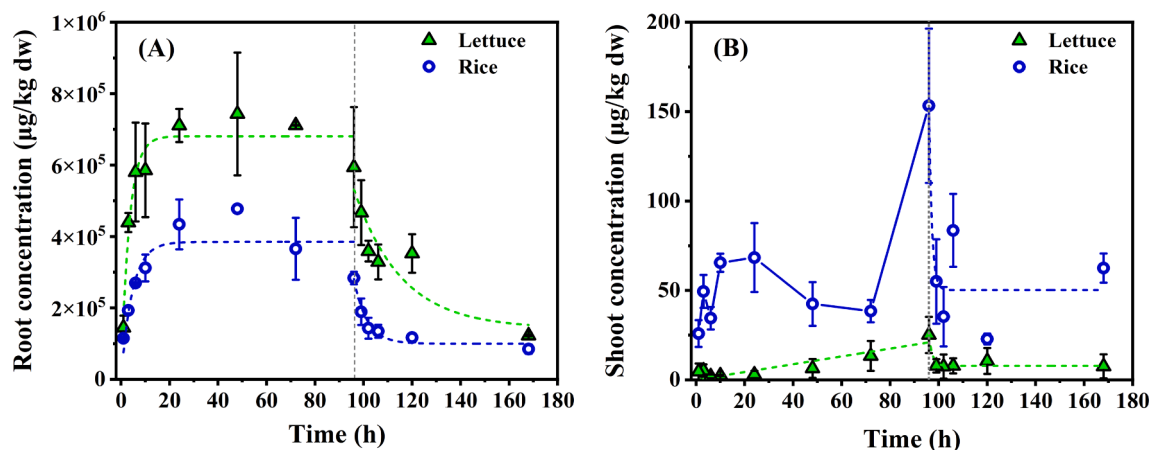

Fig. 1. Concentrations of cyetpyrafen in roots (A) and shoots (B) during the uptake and depuration period, where dw represents the dry weight. The blue and green dotted lines represent the fitting curves; the blue straight line is the point connection, and the gray dotted line indicates the switch between the uptake and elimination stages.

channels might not participate (Yu et al., 2021). The passive diffusion of organic compounds mainly relies on three interdependent properties: lipophilicity, polarity and molecular size/weight (Camenisch et al., 1998; Camenisch et al., 1996; Tommasini et al., 1998). Lipophilic xenobiotics with net neutral charge and molecular weight lower than 450 g/mol are supposed to cross lipid bilayers by passive diffusion (Kumar and Gupta, 2016; Sterling, 1994; Trapp and Mcfarlane, 1995). Based on the experimental results and chemical properties, the lipophilic and neutral uncharged cyetpyrafen (molecular weight: 393.5218 g/mol) was likely to be dominated by a passive uptake (energy-independent) process.

3.2.2. Phloem transportation pathway of cyetpyrafen

A split-root experiment was conducted to evaluate the phloem transport of cyetpyrafen in plants. The results indicated cyetpyrafen was either not detected in the rice roots growing in the unspiked solution or not found in unspiked solution (Fig. S5), demonstrating that it is difficult for cyetpyrafen to migrate from roots to shoots, and from shoots to other parts of plants via the phloem transport pathway. The strong lipophilicity of cyetpyrafen (log K_{ow} = 6.1) may lead to its fast diffusion to pass through biological membranes (Sterling, 1994); however, it could also have strong binding affinity with root lipid constituents and was not readily transported upward through the xylem system (Miller et al., 2016).

3.3. Nontarget screening and identification of cyetpyrafen metabolites

The mass distribution in the hydroponic-plant system was calculated and is presented in Fig. 2. Within 96 h of exposure, 42.3 % of spiked cyetpyrafen was lost in the plant-free controls (Fig. S6), and 69.7 % (or 61.8 %) of the total input of cyetpyrafen was depleted in the hydroponic-rice (or lettuce) system, indicating the substantial metabolism of cyetpyrafen in the hydroponic-plant system. Plant and solution extracts were thus analyzed by LC-HRMS/MS, and the acquired data were exploited by suspect and nontarget screening strategies to identify the unknown metabolites of cyetpyrafen. A total of 13 novel metabolites (M-409-1, M-409-2, M-409-3, M-409-4, M-325-1, M-325-2, M-391, M-407, M-309, M-264, M-471, M-614, and M-102) were proposed after 96 h of exposure and were not present in the control hydroponic-plant system (Table 1). All the metabolites were measured in ESI$^+$ mode and had shorter retention times than cyetpyrafen (except for M-391), indicating an increase in their polarity relative to the parent compound (HuynhReinhold, 2019). M-409-1/2/3/4 (*m/z* 409.2365) was identified as a phase I hydroxylation metabolite. The characteristic fragment ions of M-409-1 and M-409-2 were basically the same (Fig. S7). The fragments (*m/z* 57.0718, 137.0703) of M-409-1/2 were identical to those of cyetpyrafen (Fig. S8). However, the characteristic fragments (*m/z* 270.1230, 326.1859) differed from that of the parent cyetpyrafen (*m/z* 254.1280,

310.1907) by 15.995 Da (oxygen atom), indicating hydroxylation at the benzene ring. Similarly, the hydroxylation site was confirmed in M-409-3/4 by analyzing the structure of characteristic fragment ions (Figs. S9 and S10). Similarly, the structures of another two hydrolyzed metabolites (M-325-1/2) were deduced (Fig. S11 and Fig. S12). M-391 showed a loss of H$_2$ in comparison with cyetpyrafen, indicating the formation of a double bond. The characteristic fragments (Fig. S13) of *m/z* 57.0717, 109.0398, 252.1117, 290.1638 and 308.1743 elucidated its structure, which was probably formed by a dehydration reaction from M-409-4. Two characteristic fragments of *m/z* 57.0723 and 268.1112 were observed for M-407, and the proposed structure is shown in Fig. S14.

M-309 (Fig. S15) had the same fragments (*m/z* 57.0719, 109.0400, 137.0708, 183.0909, 226.0972, 254.1285) as cyetpyrafen (Fig. S8), which revealed the loss of C$_5$H$_8$O from the parent compound. The two fragments (*m/z* 145.0492, 163.0609) of the anhydroglucose moiety of M-264 (Fig. S16) subsequently corresponded to O-glycosylation of M-102. Fragmentation of M-471 (Fig. S17) exhibited five identical fragments with M-309 and cyetpyrafen. In addition, the accurate mass (*m/z* 471.2369) of M-471 was greater than that of M-309 by 162.053 Da (anhydroglucose moiety). Therefore, M-471 was identified as another glycosylated metabolite. M-614 (Fig. S18) was likely to be conjugated with glutathione because it has a mass difference of 305.068 Da (glutathione) with M-309. However, no characteristic fragments were found to support the proposed structures of M-614 and M-102 (Fig. S19), and they were marked as level 4 in terms of the reported framework (Table 1) (Schymanski et al., 2014). The structures of M-309 and M-391 were finally confirmed by synthesized standards (Figs. S20 and S21), and the retention time and characteristic fragments for synthesized standards basically coincided with those for identified metabolites in plant and solution samples.

3.4. Major transformation pathways and metabolism rules of cyetpyrafen

3.4.1. Biotranformation of cyetpyrafen in rice and lettuce

Generally, eight common transformation products (M-409-1, M-409-2, M-409-3, M-409-4, M-309, M-391, M-407 and M-102) were identified in rice roots, lettuce roots and hydroponic solutions (plant-free control). M-325-1 and M-471 were found both in rice and lettuce roots, while M-325-2, M-264 and M-614 were only detected in lettuce roots (Table 1). The metabolic pathways of cyetpyrafen in lettuce and rice roots are proposed in Fig. 3, in which ten phase I and three phase II metabolites were elucidated. Hydroxylation on different sites of cyetpyrafen led to the formation of four hydroxylated products (M-409-1/2/3/4). Subsequently, M-391 was probably generated from M-409-3 via a dehydration reaction. The formation of M-407 might originate from the intermediate of the hydroxylated metabolite (M-409-5), which was further oxidized to yield a ketone. Hydrolysis of the ester bond resulted in the generation of M-102 and M-309, where M-102 was further transformed into
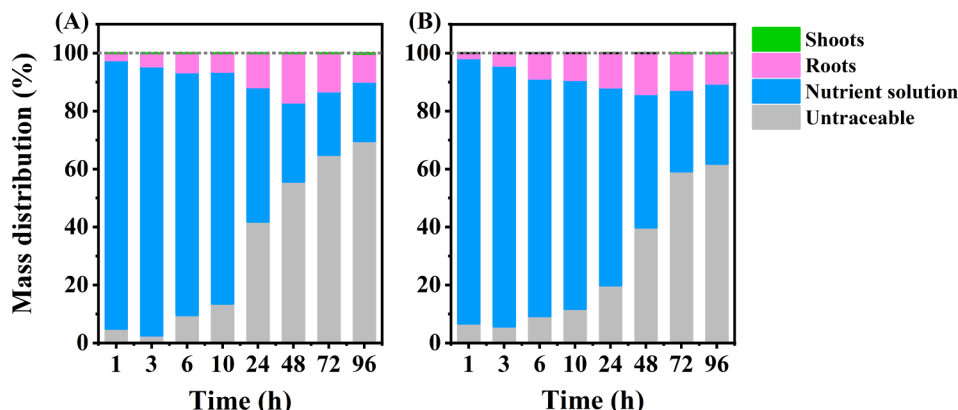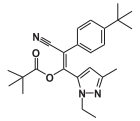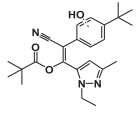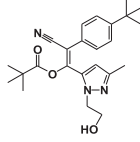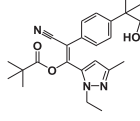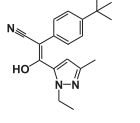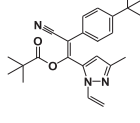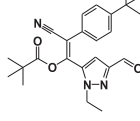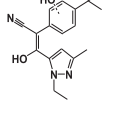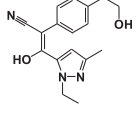

Fig. 2. Mass distribution of cyetpyrafen in hydroponic-rice (A) and hydroponic-lettuce (B) systems during 96 h of the uptake experiment.

Table 1

Structure and mass-spectral information for cyetpyrafen and its metabolites.

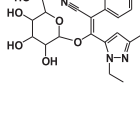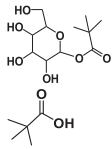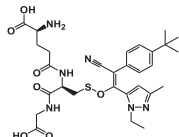| Name	Metabolic reaction	Source	Predicted formula	Retention time (min)	Accurate mass (observed $[M + H]^+$) m/z	Deviation (ppm[a])	Structure proposed	Characteristic fragments m/z	Confidence level[b]
Cyetpyrafen	—	Nutrient solution (plant-free control, hydroponic rice/lettuce system), rice/lettuce roots	$C_{24}H_{31}N_3O_2$	9.87	393.2416 (394.2480)	−2.3		310.1902, 294.1589, 254.1275, 226.0971, 184.0764, 137.0710, 109.0397, 57.0721	Level 1
M-409-1/2	Hydroxylation	Nutrient solution (plant-free control, hydroponic rice/lettuce system), rice/lettuce roots	$C_{24}H_{31}N_3O_3$	8.82/9.53	409.2365 (410.2428)	−3.4 ~ −2.4		326.1859, 270.1230, 160.0385, 137.0703, 57.0718	Level 3
M-409-3	Hydroxylation	Nutrient solution (plant-free control, hydroponic rice/lettuce system), rice/lettuce roots	$C_{24}H_{31}N_3O_3$	8.48	409.2365 (410.2435)	−0.7		392.2274, 326.1849, 308.1748	Level 2b
M-409-4	Hydroxylation	Nutrient solution (plant-free control, hydroponic rice/lettuce system), rice/lettuce roots	$C_{24}H_{31}N_3O_3$	9.78	409.2365 (410.2440)	0.5		310.1861, 294.1580, 184.0739, 109.0390	Level 2b
M-309	Hydrolysis	Nutrient solution (plant-free control, hydroponic rice/lettuce system), rice/lettuce roots	$C_{19}H_{23}N_3O$	8.61	309.1841 (310.1908)	−1.9		254.1285, 226.0972, 183.0909, 137.0708, 109.0400, 57.0719	Level 1
M-391	Hydroxylation, dehydration reaction	Nutrient solution (plant-free control, hydroponic rice/lettuce system), rice/lettuce roots	$C_{24}H_{29}N_3O_2$	10.05	391.2266 (392.2323)	−2.5		308.1743, 290.1638, 252.1117, 109.0398, 57.0717	Level 1
M-407	Hydroxylation, ketonization	Nutrient solution (plant-free control, hydroponic rice/lettuce system), rice/lettuce roots	$C_{24}H_{29}N_3O_3$	9.65	407.2209 (408.2275)	−1.7		268.1112, 57.0723	Level 2b
M-325-1	Hydrolysis, hydroxylation	Nutrient solution (hydroponic-lettuce system), rice/lettuce roots	$C_{19}H_{23}N_3O_2$	7.46	325.1790 (326.1854)	−2.8		270.1188, 216.1004, 137.0673, 109.0400	Level 3
M-325-2	Hydrolysis, hydroxylation	Lettuce roots	$C_{19}H_{23}N_3O_2$	8.52	325.1790 (326.1860)	−0.9		254.1274, 183.0893, 137.0704, 109.0402	Level 2b
M-471	Hydrolysis, glycosylation	Rice/lettuce roots	$C_{25}H_{33}N_3O_6$	6.62	471.2369 (472.2441)	−0.2		310.1905, 254.1281, 226.0999, 183.0973, 137.0696, 109.0368	Level 2b
M-264	Hydrolysis, glycosylation	Lettuce roots	$C_{11}H_{20}O_7$	4.29	264.1209 (265.1282)	0.0		163.0609, 145.0492	Level 2b

Table 1 (*continued*)

Name	Metabolic reaction	Source	Predicted formula	Retention time (min)	Accurate mass (observed [M + H]⁺) m/z	Deviation (ppm[a])	Structure proposed	Characteristic fragments m/z	Confidence level[b]
M-102	Hydrolysis	Nutrient solution (plant-free control, hydroponic rice/lettuce system), rice/lettuce roots	$C_5H_{10}O_2$	4.75	102.0681 (103.0751)	−2.6		59.0504	Level 4
M-614	Hydrolysis, glutathione conjugation	Lettuce roots	$C_{29}H_{38}N_6O_7S$	9.48	614.2523 (615.2604)	0.7		351.1218	Level 4

[a] ppm represents parts per million.
[b] Confidence levels: level 1, the structure is confirmed by a reference standard; level 2a, the spectrum data of the structure can match the data in literature or library; level 2b, the structure fits diagnostic evidence and no other structure conform with the experimental information, but the reference standard and reporting data are not available for confirmation; level 3, the evidence is not enough for one exact structure only; level 4, the formula is confirmed but the structure cannot be assigned with insufficient evidence; level 5, exact mass is obtained but the formula cannot be confirmed (Schymanski et al., 2014).
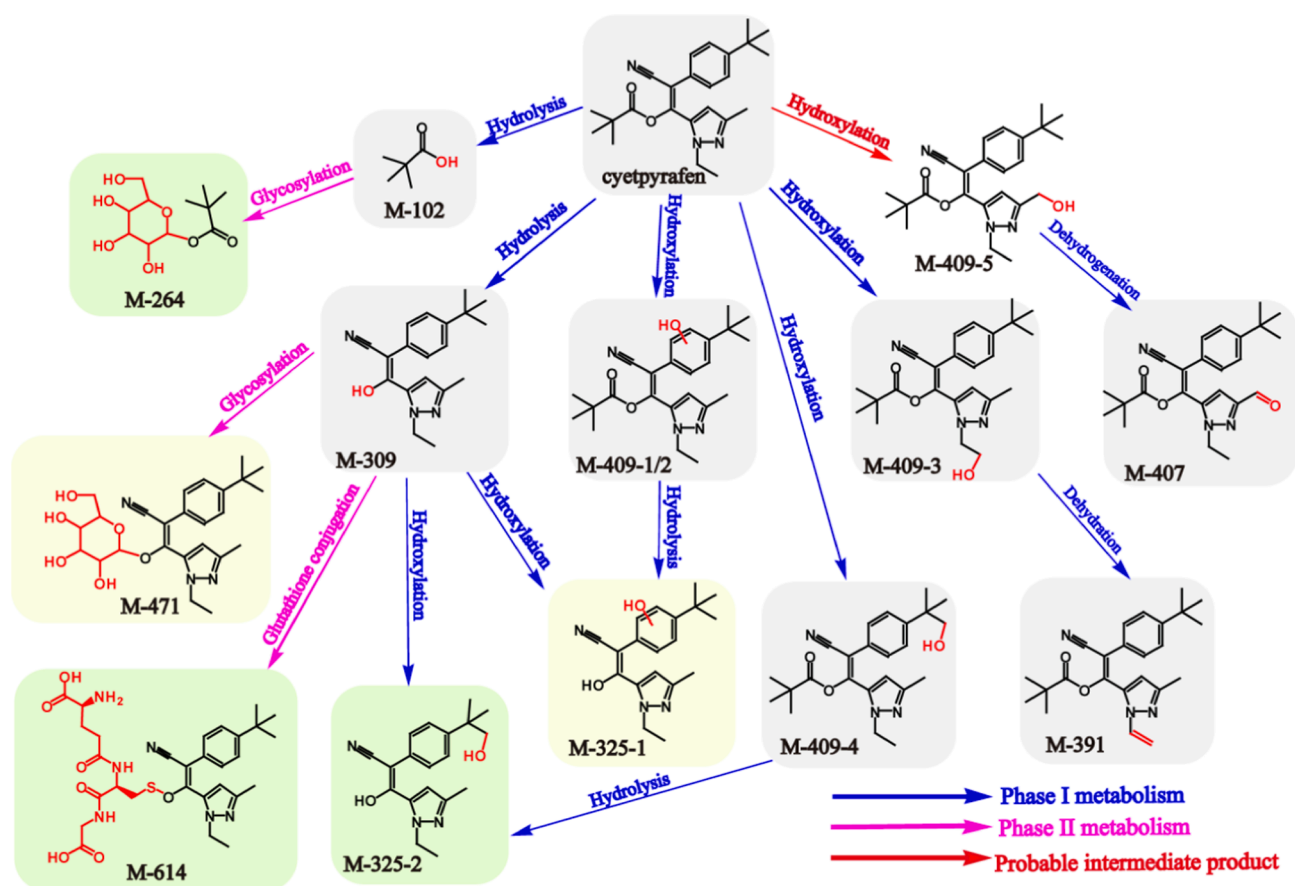
Fig. 3. Proposed transformation pathways of cyetpyrafen in the hydroponic-plant system. The blue arrow and pink arrow represent phase I and phase II reactions, respectively. The red arrow represents the reaction that produces the probable intermediate product. Compounds with the green background were only detected in lettuce, compounds with the yellow background were found in both rice and lettuce, and compounds with the gray background were discovered in hydroponic solutions in the plant-free control, rice and lettuce.

glycosylated conjugate M-264 (only in lettuce), and M-309 was further transformed into glycosylated conjugate M-471 and glutathione conjugate M-614 (only in lettuce). Conjugation with glycosides catalyzed by GT and glutathione via GST belongs to the phase II reaction, which is the main detoxification pathway of pesticides in plants (He et al., 2017). M-309 might additionally be converted to M-325-1 and M-325-2 (only in lettuce) through hydroxylation. In addition, M-325-1/2 might also be formed from M-409-1/2/4 by a hydrolysis reaction. As M-325-1/2 could only be detected in plant tissues, the reaction was possibly induced by oxidase and/or hydrolase in plants. In summary, hydroxylation, hydrolysis, dehydration, ketonization/dehydrogenation and conjugation reactions are the main transformation reactions in plants. These results indicated that the metabolic behavior of cyetpyrafen might vary between rice and lettuce in terms of the possible differences in pathways and metabolites, or probably the levels of M-325-2, M-264 and M-614 in rice roots were too low to be detected.

As reference standards were not available for most of the newly identified metabolites, considering their similar core structures and the use of the same analytical conditions, peak areas were applied for their relative quantification. The relative areas of these metabolites in the hydroponic-plant system and plant-free control are presented in Fig. 4. The results suggested that M-409 (m/z 409.2365), M-309 and M-391 were the main metabolites in both the hydroponic solution and roots. After 96 h of exposure, the sum of their peak areas accounted for 84.6 % of all identified metabolites in the hydroponic solution in the plant-free control, 95.9 % (or 84.2 %) and 96.0 % (or 87.9 %) in the liquid phase and roots in the hydroponic-rice (or lettuce) system, respectively. Although the metabolites in nutrient solutions may be partly enriched in roots, the MS response of M-409 and M-309 in solution from the hydroponic-plant system was still higher than that from the plant-free control after 24 h and 48 h of exposure (Fig. S22). The results further proved that oxidation and hydrolysis reactions of cyetpyrafen (M-409 and M-309) occurred in both the hydroponic solution and plant roots. Therefore, abiotic and biological transformation may both be involved in the oxidation and ester hydrolysis of cyetpyrafen in plants. In addition, the peak areas of the glycosylated metabolite M-471 decreased gradually after 24 h of exposure in lettuce roots (Fig. S22), suggesting that it was further converted (e.g., malonylated) or incorporated into

cell components. However, metabolites were not detected in the shoots of rice and lettuce mainly because of the trace accumulation of cyetpyrafen in shoots as well as the poor translocation capacity of metabolites from roots to shoots.

3.4.2. Transformation of cyetpyrafen in hydroponic solution

After 168 h of exposure, 44.5 % of the initial input of cyetpyrafen declined in the plant-free controls, indicating its substantial abiotic transformation in the hydroponic solution (Fig. S6). As shown in Fig. 3, eight abiotic transformation products (M-409-1, M-409-2, M-409-3, M-409-4, M-309, M-391, M-407 and M-102) were identified in hydroponic solutions (plant-free control). Transformation reactions, including hydroxylation, ketonization/dehydrogenation, dehydration and hydrolysis, were proposed (Fig. 3). Carbon hydroxylation and ketonization of cyetpyrafen might be induced by free radicals (HO· and CO$_3^-$) in the solution, as these radicals were found to mediate the hydroxylation and ketonization reactions of pharmaceuticals such as naproxen (Luo et al., 2018; Zhou et al., 2020). The carbon atom (electrophilic group) connected by the ester bond might be attacked by nucleophilic H$_2$O or OH$^-$ in aqueous solution, leading to the hydrolysis of cyetpyrafen through a bimolecular nucleophilic substitution reaction (Li et al., 2020b).

Interestingly, M-325-1 could only be detected in the solution from the hydroponic-plant system rather than the plant-free controls (Fig. S22). Plant roots can exude enzymes such as POD, dehydrogenase and hydrolases that can accelerate the transformation of pesticides, which may catalyze the oxidation and hydrolysis reactions of cyetpyrafen and generate metabolites such as M-325-1 (He et al., 2017; LeFevre et al., 2016; Wang et al., 2014).

3.5. Plant enzymatic response

To explore the possible biotransformation mechanism of cyetpyrafen in plants, the activities of detoxification enzymes including CYP450, POD, CarE, GT and GST in the roots of the treated and untreated groups were measured. As shown in Fig. 5 and Fig. S23, during 96 h of exposure, the activity of CYP450, POD, CarE, GT and GST in cyetpyrafen treated rice (or lettuce) roots was up to 1.6 (or 1.7), 1.8 (or 2.3), 1.6 (or 2.1), 1.7 (or 2.0) and 1.6 (or 1.4) times higher than that in control rice (or lettuce)
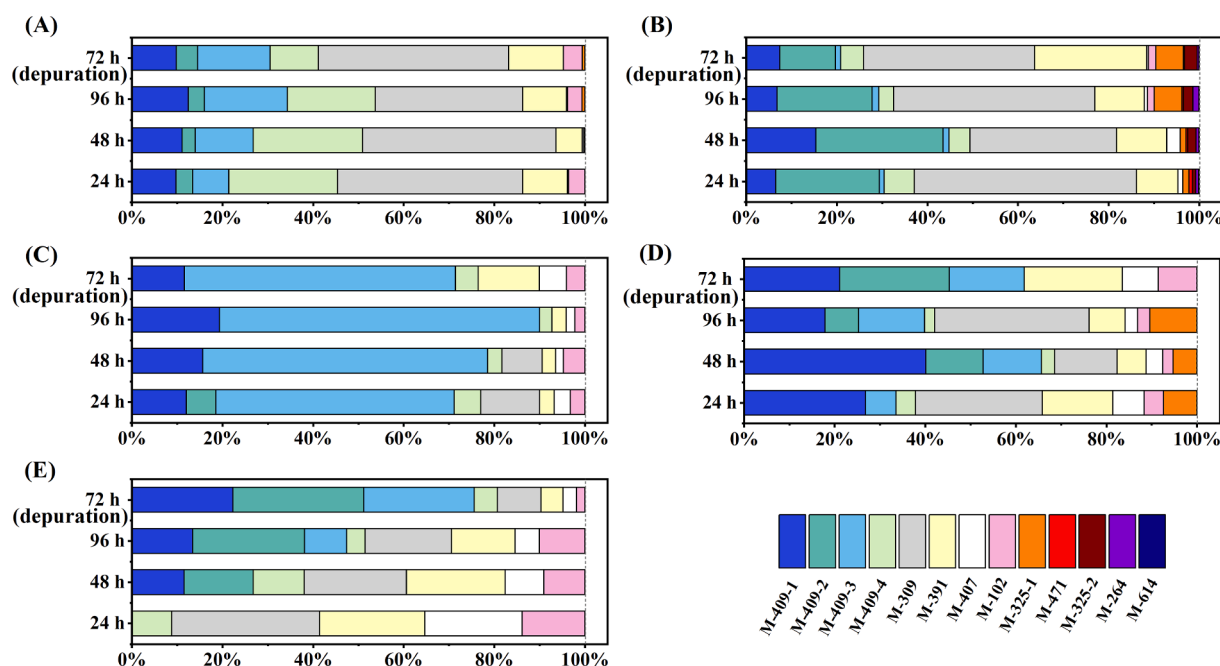

Fig. 4. Relative peak areas of the metabolites of cyetpyrafen in rice roots (A), lettuce roots (B), nutrient solution in hydroponic-rice system (C), nutrient solution in hydroponic-lettuce system (D) and nutrient solution in plant-free control (E) at 24 h, 48 h and 96 h of uptake stage and 72 h of depuration stage.
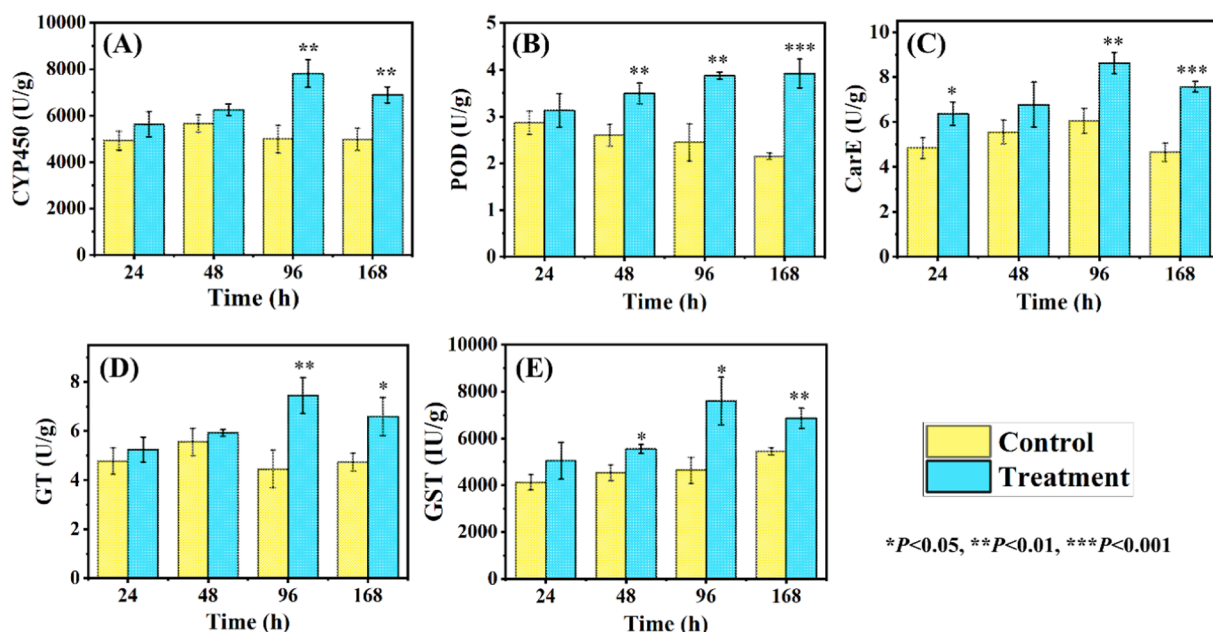
Fig. 5. Enzyme activities of CYP450 (A), POD (B), CarE (C), GT (D) and GST (E) in rice roots at different exposure times. The yellow columns represent enzyme activities in the control group, and the blue columns represent enzyme activities in the treatment group. Significant differences in enzyme activities between the control and treatment groups were compared by one-way ANOVA. Levels of significant difference between the two groups were denoted as: $*P < 0.05$, $**P < 0.01$, $***P < 0.001$.

roots (without cyetpyrafen), respectively. The increases in enzyme activities were consistent with the presence of relevant metabolites, indicating that these enzymes are probably involved in the plant metabolism of cyetpyrafen. CYP450 catalyzes many reactions, including hydroxylation, dehydration, and dehydrogenation (Van Eerd et al., 2003). For example, cyenopyrafen is a structural analog of cyetpyrafen, and Riga et al. (2015) reported that CYP392A11, a cytochrome P450 in *Tetranychus urticae*, could catalyze cyenopyrafen to hydroxylated cyenopyrafen. POD is another oxidative enzyme that can mediate ring hydroxylation of pesticides (Huang et al., 2013; Van Eerd et al., 2003). POD enzymes also participate in phase III metabolism in plants, which promote the formation of bound residues (Van Eerd et al., 2003). These oxidative enzymes may take part in the formation of M-409-1/2/3/4, M-407, M-391 and M-325-1/2. CarE could catalyze the hydrolyzation reaction of the ester bond of the pesticides (Cummins and Edwards, 2004), which might be responsible for the generation of hydrolyzed products (M-309, M-102 and M-325-1/2). GT and GST could mediate the conjugation reaction with glycoside and glutathione, respectively

(Ravichandran and Philip, 2021); accordingly, they may contribute to the formation of two glycosylated conjugates (M-471, M-264) and one glutathione conjugate (M-614) after phase I reactions. It should be noted that the activation of some plant enzymes (i.e., GST and POD) activities might also be caused by oxidative stress of cyetpyrafen because GST and POD are also considered to participate in oxidative stress responses of xenobiotics (Edwards et al., 2000; Passardi et al., 2005).

3.6. Toxicity prediction of cyetpyrafen and metabolites

Computerized predictive toxicology is an effective approach for potential toxicity screening that can avoid killing animals and has been widely used to facilitate the toxicity evaluation of new chemicals (Gao et al., 2019; Ma et al., 2021; Maunz et al., 2013). In this study, the ecotoxicity of cyetpyrafen and its metabolites were predicted by ECO-SAR based on their structures. According to the classification of ecotoxicity (S6), cyetpyrafen was estimated to be very toxic to fish (chronic toxicity: chronic value ≤ 0.01 mg/L, acute toxicity: $LC_{50} \leq 1$ mg/L). The

Table 2
Predicted log K_{ow}, chronic and acute toxicity of cyetpyrafen and its metabolites to nontargeted organisms by ECOSAR.

Compound name	log K_{ow}	Chronic toxicity (chronic value, mg a.i./L)				Acute toxicity (mg a.i./L)		
		Fish	Daphnid	Green algae		Fish (96 h LC_{50})	Daphnid (48 h EC_{50})	Green algae (96 h EC_{50})
cyetpyrafen	6.1	0.01	0.02*	0.12*		0.06*	0.05*	0.19*
M-391	6.0	0.01	0.02*	0.14*		0.09*	0.07*	0.24*
M-409-1/2	5.6	0.03	0.04	0.24*		0.18*	0.14*	0.43*
M-407	5.3	0.05*	0.07*	0.38*		0.37*	0.29*	0.75*
M-409-3/4	4.7	0.18*	0.19*	0.93*		1.38*	1.00*	2.06*
M-309	4.3	0.29	0.28	1.19		2.29*	1.60*	2.85*
M-325-1	3.8	0.77	0.67	2.44		6.50	4.36	6.44
M-325-2	3.2	2.40	1.82	5.45		21.48*	13.65*	16.19*
M-471	1.9	47.62*	26.23*	50.48*		493.42*	277.15*	197.43*
M-264	−1.3	14714.73	3735.42	2478.93		2.17×10^5	90342.98	18808.54
M-614	−1.7	73683.99*	17025.45*	9927.90*		$1.13 \times 10^{6*}$	$4.55 \times 10^{5*}$	81639.45*
M-102	1.4	–	–	–		–	–	–

LC_{50}: median lethal concentration.
EC_{50}: median effective concentration.
   * : chemical may not be soluble enough to measure this predicted effect.

acute toxicity of cyetpyrafen was found to be highly toxic toward daphnid and green algae, and its chronic toxicity was observed to be toxic and harmful toward these two species (Table 2). Regarding the transformation products, M-391, M-409-1, M-409-2 and M-407 showed almost the same level of ecotoxicity as the parent cyetpyrafen. The toxic levels of M-409-3, M-409-4, M-309 and M-325-1 were classified as toxic, and M-325-2 was harmful to aquatic organisms on the basis of acute toxicity. Considering the high production of M-409 and M-391 as well as their high potential toxicity, these metabolites should also be specifically considered when evaluating the ecotoxicity of cyetpyrafen. However, their ecotoxicity merits future experimental tests to obtain solid data. Three phase II metabolites (M-471, M-264 and M-614) were estimated to be not harmful to aquatic organisms, probably because the phase II reaction is the main procedure in the detoxification of xenobiotics (Van Eerd et al., 2003).

4. Implications

As new man-made agrochemicals have been kept introduced into agricultural environments, they may pose threats to ecosystems and human health through food chain transfer after plant uptake. In this study, within only 96 h of exposure, the rapid uptake, great bioaccumulation and extensive transformation of the novel pesticide cyetpyrafen in hydroponic-plant systems further highlighted the importance of examining plant uptake and metabolism to comprehensively assess the potential risks of new agrochemicals. One limitation of this study is that the hydroponic setting may not well reflect the fate of cyetpyrafen in the soil–plant system under field conditions. However, these results could provide essential data for comprehensively assessing cyetpyrafen accumulation and metabolism in crops, and the research strategy could also set as an example for exploring the fate of other new agrochemicals in crops.

Transformation of pesticides plays a key role in modulating their overall toxicity and accumulation, and ignoring metabolized fractions of pesticides in plants may underestimate the extent of human exposure and potential adverse impacts. Some metabolites of pesticides possess bioactivity/toxicity equivalent or greater than that of their parent (Cui et al., 2019; Mahajna et al., 1997; Seifrtova et al., 2017; Xie et al., 2019; Zhang et al., 2020; Zhao et al., 2017), and some metabolites can be readily back-transformed to their parent via deconjugation/demethylation/remethylation reactions (Cheng et al., 2021; Fu et al., 2020; Fu et al., 2018; Shi et al., 2009). In this study, as many as 13 biotic/abiotic transformation products of cyetpyrafen were identified in hydroponic-plant systems for the first time. Interestingly, the most abundant metabolites (M-391 and M-409) of cyetpyrafen were estimated to have ecotoxicity similar to that of the parent. After human ingestion, glycosylated conjugates might be deconjugated via hydrolyzation (Devasena and Menon, 2003; Koppel et al., 2017). Therefore, further research is warranted to identify the plant transformation products of pesticides as well as their fate and toxicity after application, both to more accurately evaluate their effects on human health and to develop predictive risk assessment models, especially for new agrochemicals.

CRediT authorship contribution statement

Runan Li: Investigation, Data curation, Writing – original draft. **Sijia Wang:** Methodology, Validation. **Jinhe Chang:** Investigation, Writing – review & editing. **Xinglu Pan:** Formal analysis. **Fengshou Dong:** Writing – review & editing, Supervision. **Zhiyuan Li:** Software. **Yongquan Zheng:** Writing – review & editing. **Yuanbo Li:** Conceptualization, Writing – review & editing, Project administration, Funding acquisition.

Declaration of Competing Interest

The authors declare that they have no known competing financial interests or personal relationships that could have appeared to influence the work reported in this paper.

Data availability

Data will be made available on request.

Appendix A. Supplementary data

Additional description and data about chemicals and reagents, enzyme assays, analysis method, classification of ecotoxicity, effects of inhibitors on root uptake, accumulation and elimination parameters, BCF values and TF values in the plant uptake experiment, concentration and dissipation kinetics of cyetpyrafen in nutrient solution, chemical structure of cyetpyrafen, chromatogram and fragmentation spectra of cyetpyrafen and its metabolites, temporal variation of the peak areas of the metabolites are provided in the supplementary material. Supplementary data to this article can be found online at https://doi.org/10.10 16/j.envint.2022.107522.

References

Aktar, M.W., Sengupta, D., Chowdhury, A., 2009. Impact of pesticides use in agriculture: their benefits and hazards. Interdiscip. Toxicol. 2, 1–12.

Bromilow, R.H., Chamberlain, K., Tench, A.J., Williams, R.H., 1993. Phloem translocation of strong acids glyphosate, substituted phosphonic and sulfonic-acids in *Ricinus communis* L. Pestic. Sci. 37 (1), 39–47.

Camenisch, G., Folkers, G., van de Waterbeemd, H., 1996. Review of theoretical passive drug absorption models: Historical background, recent developments and limitations. Pharm. Acta Helv. 71, 309–327.

Camenisch, G., Alsenz, J., Waterbeemd, H.V.D., Folkers, G., 1998. Estimation of permeability by passive diffusion through Caco-2 cell monolayers using the drugs' lipophilicity and molecular weight. Eur. J. of Pharm. Sci. 6, 313–319.

Chen, J.C., Gong, Y.J., Shi, P., Wang, Z.H., Cao, L.J., Wang, P., Wei, S.J., 2019a. Field-evolved resistance and cross-resistance of the two-spotted spider mite, *Tetranychus urticae*, to bifenazate, cyenopyrafen and SYP-9625. Exp. Appl. Acarol. 77 (4), 545–554.

Chen, X.C., Li, Y.X., Jiang, L.S., Hu, B.Y., Wang, L., An, S.Y., Zhang, X.L., 2021. Uptake, accumulation, and translocation mechanisms of steroid estrogens in plants. Sci. Total Environ. 753, 141979.

Chen, Y., Lu, Y.H., Nie, E.G., Akhtar, K., Zhang, S.F., Ye, Q.F., Wang, H.Y., 2020. Uptake, translocation and accumulation of the fungicide benzene kresoxim-methyl in Chinese flowering cabbage (*Brassica campastris* var. *parachinensis*) and water spinach (*Ipomoea aquatica*). Environ. Pollut. 264, 114815.

Chen, K.Y., Tian, F.J., Wu, C., Wu, X.H., Xu, J., Dong, F.S., Liu, X.G., Zheng, Y.Q., 2019b. Degradation products and pathway of ethiprole in water and soil. Water Res. 161, 531–539.

Cheng, Z., Sun, H., Sidhu, H.S., Sy, N.D., Wang, X., Gan, J., 2021. Conjugation of di-n-butyl phthalate metabolites in *Arabidopsis thaliana* and potential deconjugation in human microsomes. Environ. Sci. Technol. 55 (4), 2381–2391.

Cheng, X., Wang, Y., Huang, L., Xu, P., Zhang, S., Ye, Q., 2022. Behavior and fate of a novel neonicotinoid cycloxaprid in water–sediment systems through position-specific C-14 labeling. Chem. Eng. J. 435, 134962.

Chuang, Y.H., Liu, C.H., Sallach, J.B., Hammerschmidt, R., Zhang, W., Boyd, S.A., Li, H., 2019. Mechanistic study on uptake and transport of pharmaceuticals in lettuce from water. Environ. Int. 131, 104976.

Coleman, J.O.D., BlakeKalff, M.M.A., Davies, T.G.E., 1997. Detoxification of xenobiotics by plants: Chemical modification and vacuolar compartmentation. Trends Plant Sci. 2 (4), 144–151.

Cui, J.N., Wang, F., Gao, J., Zhai, W.J., Zhou, Z.Q., Liu, D.H., Wang, P., 2019. Bioaccumulation and metabolism of carbosulfan in zebrafish (*Danio rerio*) and the toxic effects of its metabolites. J. Agric. Food Chem. 67 (45), 12348–12356.

Cummins, I., Edwards, R., 2004. Purification and cloning of an esterase from the weed black-grass (*Alopecurus myosuroides*), which bioactivates aryloxyphenoxypropionate herbicides. Plant J. 39 (6), 894–904.

Devasena, T., Menon, V.P., 2003. Fenugreek affects the activity of beta-glucuronidase and mucinase in the colon. Phytother. Res. 17 (9), 1088–1091.

Edwards, R., Dixon, D.P., Walbot, V., 2000. Plant glutathione S-transferases: enzymes with multiple functions in sickness and in health. Trends Plant Sci. 5, 193–198.

Feng, Y.J., Zhang, L.S., Chen, H.Y., Wang, M.Q., Liu, C.X., Li, Y.Y., Song, Y.Q., Mao, J.J., 2021. Contact toxicity of a new acaricide, SYP-9625, to the natural predator, *Chrysopa pallens*. J. Asia-Pac. Entomol. 24 (2), 125–130.

Fu, Q.L., Blaney, L., Zhou, D.M., 2016. Phytotoxicity and uptake of roxarsone by wheat (*Triticum aestivum* L.) seedlings. Environ. Pollut. 219, 210–218.

Fu, Q., Liao, C., Du, X., Schlenk, D., Gan, J., 2018. Back conversion from product to parent: Methyl triclosan to triclosan in plants. Environ. Sci. Technol. Lett. 5 (3), 181–185.

Fu, Q., Fedrizzi, D., Kosfeld, V., Schlechtriem, C., Ganz, V., Derrer, S., Rentsch, D., Hollender, J., 2020. Biotransformation changes bioaccumulation and toxicity of diclofenac in aquatic organisms. Environ. Sci. Technol 54 (7), 4400–4408.

Gao, Y.P., Li, G.Y., Qin, Y.X., Ji, Y.M., Mai, B.X., An, T.C., 2019. New theoretical insight into indirect photochemical transformation of fragrance nitro-musks: Mechanisms, eco-toxicity and health effects. Environ. Int. 129, 68–75.

Gong, X., Wang, Y., Pu, J., Zhang, J., Sun, H., Wang, L., 2020. The environment behavior of organophosphate esters (OPEs) and di-esters in wheat (*Triticum aestivum* L.): Uptake mechanism, in vivo hydrolysis and subcellular distribution. Environ. Int. 135, 105405.

He, Y.J., Langenhoff, A.A.M., Sutton, N.B., Rijnaarts, H.H.M., Blokland, M.H., Chen, F.R., Huber, C., Schroder, P., 2017. Metabolism of ibuprofen by *Phragmites australis*: uptake and phytodegradation. Environ. Sci. Technol. 51 (8), 4576–4584.

Huang, H., Zhang, S., Wang, S., Lv, J., 2013. In vitro biotransformation of PBDEs by root crude enzyme extracts: Potential role of nitrate reductase (NaR) and glutathione S-transferase (GST) in their debromination. Chemosphere 90 (5), 1885–1892.

Hurtado, C., Trapp, S., Bayona, J.M., 2016. Inverse modeling of the biodegradation of emerging organic contaminants in the soil-plant system. Chemosphere 156, 236–244.

Huynh, K., Reinhold, D., 2019. Metabolism of sulfamethoxazole by the model plant *Arabidopsis thaliana*. Environ. Sci. Technol. 53 (9), 4901–4911.

Ju, C., Li, X., He, S., Shi, L., Yu, S., Wang, F., Xu, S., Cao, D., Fang, H., Yu, Y., 2020. Root uptake of imidacloprid and propiconazole is affected by root composition and soil characteristics. J. Agric. Food Chem. 68 (52), 15381–15389.

Khalighi, M., Tirry, L., Van Leeuwen, T., 2014. Cross-resistance risk of the novel complex II inhibitors cyenopyrafen and cyflumetofen in resistant strains of the two-spotted spider mite *Tetranychus urticae*. Pest Manag. Sci. 70 (3), 365–368.

Koppel, N., Rekdal, V.M., Balskus, E.P., 2017. Chemical transformation of xenobiotics by the human gut microbiota. Science 356 (6344), 1246–1257.

Kumar, K., Gupta, S.C., 2016. A framework to predict uptake of trace organic compounds by plants. J. Environ. Qual. 45, 555–564.

LeFevre, G.H., Portmann, A.C., Müller, C.E., Sattely, E.S., Luthy, R.G., 2016. Plant assimilation kinetics and metabolism of 2-mercaptobenzothiazole tire rubber vulcanizers by *Arabidopsis*. Environ. Sci. Technol. 50 (13), 6762–6771.

Li, J., Hu, T., Wang, G., Nie, P., Xiao, H., Shang, S., 2020a. Virulence and field control efficacy of nine acaricides against two-spotted spider mite *Tetranychus urticae* in strawberry. Acat Agriculturae Boreali-Occidentalis Sinica 29 (6), 921–927.

Li, L.Z., Tu, C., Peijnenburg, W., Luo, Y.M., 2017. Characteristics of cadmium uptake and membrane transport in roots of intact wheat (*Triticum aestivum* L.) seedlings. Environ. Pollut. 221, 351–358.

Li, M.M., Wang, R., Kong, Z.Q., Gao, T.F., Wang, F.Z., Fan, B., 2020b. Cyflumetofen degradation in different aquatic environments and identification of hydrolytic products. J. Environ. Chem. Eng 8 (6), 104512.

Lin, T., Zeng, Z.H., Chen, Y.X., You, Y., Hu, J.F., Yang, F.H., Wei, H., 2021. Compatibility of six reduced-risk insecticides with *Orius strigicollis* (Heteroptera: Anthocoridae) predators for controlling *Thrips hawaiiensis* (Thysanoptera: Thripidae) pests. Ecotoxicol. Environ. Saf. 226, 112812.

Liu, Q., Wang, X., Yang, R., Yang, L., Sun, B., Zhu, L., 2019. Uptake kinetics, accumulation, and long-distance transport of organophosphate esters in plants: impacts of chemical and plant properties. Environ. Sci. Technol. 53, 4940–4947.

Luo, S., Gao, L.W., Wei, Z.S., Spinney, R., Dionysiou, D.D., Hu, W.P., Chai, L.Y., Xiao, R. Y., 2018. Kinetic and mechanistic aspects of hydroxyl radical-mediated degradation of naproxen and reaction intermediates. Water Res. 137, 233–241.

Ma, C., Liu, X., Wu, X., Dong, F., Xu, J., Zheng, Y., 2021. Kinetics, mechanisms and toxicity of the degradation of imidaclothiz in soil and water. J. Hazard. Mater. 403, 124033.

Mahajna, M., Quistad, G.B., Casida, J.E., 1997. Acephate insecticide toxicity: Safety conferred by inhibition of the bioactivating carboxyamidase by the metabolite methamidophos. Chem. Res. Toxicol. 10 (1), 64–69.

Malchi, T., Eyal, S., Czosnek, H., Shenker, M., Chefetz, B., 2021. Plant pharmacology: Insights into in-planta kinetic and dynamic processes of xenobiotics. Crit. Rev. in Environ. Sci. Technol. DOI: 10.1080/10643389.2021.1946360.

Maunz, A., Gütlein, M., Rautenberg, M., Vorgrimmler, D., Gebele, D., Helma, C., 2013. lazar: a modular predictive toxicology framework. Front. Pharmacol. 4 (38), 1–10.

Miller, E.L., Nason, S.L., Karthikeyan, K.G., Pedersen, J.A., 2016. Root uptake of pharmaceuticals and personal care product ingredients. Environ. Sci. Technol. 50 (2), 525–541.

Naidu, R., Biswas, B., Willett, I.R., Cribb, J., Kumar Singh, B., Paul Nathanail, C., Coulon, F., Semple, K.T., Jones, K.C., Barclay, A., Aitken, R.J., 2021. Chemical pollution: A growing peril and potential catastrophic risk to humanity. Environ. Int. 156, 106616.

Ouyang, J.Q., Tian, Y.J., Jiang, C.X., Yang, Q.F., Wang, H.J., Li, Q., 2018. Laboratory assays on the effects of a novel acaricide, SYP-9625 on *Tetranychus cinnabarinus*

(Boisduval) and its natural enemy, *Neoseiulus californicus* (McGregor). PLoS ONE 13 (11), 1–20.

Passardi, F., Cosio, C., Penel, C., Dunand, C., 2005. Peroxidases have more functions than a Swiss army knife. Plant Cell Rep. 24, 255–265.

Qiu, J., Chen, G., Xu, J., Luo, E., Liu, Y., Wang, F., Zhou, H., Liu, Y., Zhu, F., Ouyang, G., 2016. In vivo tracing of organochloride and organophosphorus pesticides in different organs of hydroponically grown malabar spinach (*Basella alba* L.). J. Hazard. Mater. 316, 52–59.

Ravichandran, M.K., Philip, L., 2021. Insight into the uptake, fate and toxic effects of pharmaceutical compounds in two wetland plant species through hydroponics studies. Chem. Eng. J. 426, 131078.

Riemenschneider, C., Seiwert, B., Moeder, M., Schwarz, D., Reemtsma, T., 2017. Extensive transformation of the pharmaceutical carbamazepine following uptake into intact tomato plants. Environ. Sci. Technol. 51 (11), 6100–6109.

Riga, M., Myridakis, A., Tsakireli, D., Morou, E., Stephanou, E.G., Nauen, R., Van Leeuwen, T., Douris, V., Vontas, J., 2015. Functional characterization of the *Tetranychus urticae* CYP392A11, a cytochrome P450 that hydroxylates the METI acaricides cyenopyrafen and fenpyroximate. Insect Biochem. Mol. Biol. 65, 91–99.

Romeh, A.A., Hendawi, M.Y., 2013. Chlorpyrifos insecticide uptake by plantain from polluted water and soil. Environ. Chem. Lett. 11, 163–170.

Schymanski, E.L., Jeon, J., Gulde, R., Fenner, K., Ruff, M., Singer, H.P., Hollender, J., 2014. Identifying small molecules via high resolution mass spectrometry: communicating confidence. Environ. Sci. Technol. 48 (4), 2097–2098.

Seifrtova, M., Halesova, T., Sulcova, K., Riddellova, K., Erban, T., 2017. Distributions of imidacloprid, imidacloprid-olefin and imidacloprid-urea in green plant tissues and roots of rapeseed (*Brassica napus*) from artificially contaminated potting soil. Pest Manag. Sci. 73 (5), 1010–1016.

Shao, S., Cheng, X., Zheng, R., Zhang, S., Yu, Z., Wang, H., Wang, W., Ye, Q., 2022. Sex-related deposition and metabolism of vanisulfane, a novel vanillin-derived pesticide, in rats and its hepatotoxic and gonadal effects. Sci. Total Environ. 813, 152545.

Shao, X., Swenson, T.L., Casida, J.E., 2013. Cycloxaprid insecticide: nicotinic acetylcholine receptor binding site and metabolism. J. Agric. Food Chem. 61, 7883–7888.

Shen, D., Lu, Z., Zhong, J., Zhang, S., Ye, Q., Wang, W., Gan, J., 2021. Combination of high specific activity carbon-14 labeling and high resolution mass spectrometry to study pesticide metabolism in crops: Metabolism of cycloxaprid in rice. Environ. Int. 157, 106879.

Shi, X., Dick, R.A., Ford, K.A., Casida, J.E., 2009. Enzymes and inhibitors in neonicotinoid insecticide metabolism. J. Agric. Food Chem. 57 (11), 4861–4866.

Sicbaldi, F., Sacchi, G.A., Trevisan, M., Del Re, A.A.M., 1997. Root uptake and xylem translocation of pesticides from different chemical classes. Pestic. Sci. 50, 111–119.

Sterling, T.M., 1994. Mechanisms of herbicide absorption across plant membranes and accumulation in Plant Cells. Weed Sci. 42, 263–276.

Tommasini, R., Vogt, E., Fromenteau, M., Hörtensteiner, S., Matile, P., Amrhein, N., Martinoia, E., 1998. An ABC-transporter of *Arabidopsis thaliana* has both glutathione-conjugate and chlorophyll catabolite transport activity. The Plant J. 13, 773–780.

Trapp, S., 2000. Modelling uptake into roots and subsequent translocation of neutral and ionisable organic compounds. Pest. Manag. Sci. 56, 767–778.

Trapp, S., Farlane, J.C.M., 1995. Plant contamination: Modeling and simulation of organic chemical processes. CRC Press, Boca Raton, FL.

Van Eerd, L.L., Hoagland, R.E., Zablotowicz, R.M., Hall, J.C., 2003. Pesticide metabolism in plants and microorganisms. Weed Sci. 51 (4), 472–495.

Wang, Y., Fang, L., Lin, L., Luan, T., Tam, N.F.Y., 2014. Effects of low molecular-weight organic acids and dehydrogenase activity in rhizosphere sediments of mangrove plants on phytoremediation of polycyclic aromatic hydrocarbons. Chemosphere 99, 152–159.

Wang, Z.N., Meng, Y.X., Mei, X.D., Ning, J., Ma, X.D., She, D.M., 2020. Assessment of handler exposure to pesticides from stretcher-type power sprayers in orchards. Appl. Sci.-Basel 10 (23), 11.

Wildeman, A.G., Nazar, R.N., 1982. Significance of plant metabolism in the mutagenicity and toxicity of pesticides. Can. J. Genet. Cytol. 24 (4), 437–449.

Xie, Y., Jiang, H.T., Chang, J., Wang, Y.H., Li, J.Z., Wang, H.L., 2019. Gonadal disruption after single dose exposure of prothioconazole and prothioconazole-desthio in male lizards (*Eremias argus*). Environ. Pollut. 255, 113297.

Yu, H.B., Cheng, Y., Xu, M., Song, Y.Q., Luo, Y.M., Li, B., 2016. Synthesis, acaricidal activity, and structure-activity relationships of pyrazolyl acrylonitrile derivatives. J. Agric. Food Chem. 64 (51), 9586–9591.

Yu, P.F., Li, Y.W., Zou, L.J., Liu, B.L., Xiang, L., Zhao, H.M., Li, H., Cai, Q.Y., Hou, X.W., Mo, C.H., Wong, M.H., Li, Q.X., 2021. Variety-selective rhizospheric activation, uptake, and subcellular distribution of perfluorooctanesulfonate (PFOS) in lettuce (*Lactuca sativa* L.). Environ. Sci. Technol. 55 (13), 8730–8741.

Zhang, Z.X., Zhang, J., Zhao, X.J., Gao, B.B., He, Z.Z., Li, L.S., Shi, H.Y., Wang, M.H., 2020. Stereoselective uptake and metabolism of prothioconazole caused oxidative stress in zebrafish (*Danio rerio*). J. Hazard. Mater. 396, 122756.

Zhao, Y.Y., Wendling, L.A., Wang, C.H., Pei, Y.S., 2017. Behavior of chlorpyrifos and its major metabolite TCP (3,5,6-trichloro-2-pyridinol) in agricultural soils amended with drinking water treatment residuals. J. Soils and Sediments 17 (4), 889–900.

Zhou, Y.J., Chen, C.Y., Guo, K.H., Wu, Z.H., Wang, L.P., Hua, Z.C., Fang, J.Y., 2020. Kinetics and pathways of the degradation of PPCPs by carbonate radicals in advanced oxidation processes. Water Res. 185, 116231.